



National
Defence

Défense
nationale

PULSE-WIDTH DEPENDENT RADIATION EFFECTS ON ELECTRONIC COMPONENTS

by

T. Cousins
*Nuclear Effects Section
Electronics Division*

DTIC
ELECTE
MAR 26 1990
S B D

DEFENCE RESEARCH ESTABLISHMENT OTTAWA
TECHNICAL NOTE 89-33

PCN
041LS

November 1989
Ottawa

DISTRIBUTION STATEMENT A

Approved for public release;
Distribution Unlimited

ABSTRACT

The simulation of the prompt gamma-ray pulse effects on electronics with an electron linear accelerator (LINAC) has been performed by DREO and other groups. However, the use of a LINAC normally entails wider pulses than those expected on the battlefield. This report examines the effects of the variation of pulse width on electronic response using both theoretical and experimental examples. The conclusions are that pulse-width fidelity is important for a number of possible scenarios, and that for complete understanding of electronic performance, a variable pulse-width simulator is essential.

RÉSUMÉ

La simulation de l'action des rayons gamma rapides sur les composantes électroniques à l'aide d'un accélérateur linéaire (LINAC) a été réalisée par le CRDO et d'autres groupes. Par contre, l'emploi du LINAC donne normalement des impulsions plus larges que celles normalement éprouvées sur un champ de bataille. Ce rapport examine les effets de la variation de la largeur des impulsions sur les composantes électroniques en se servant d'exemples théoriques et expérimentaux. Les conclusions sont que la précision de la largeur des impulsions est très importante pour un nombre possible de scénarios et que pour une compréhension complète du rendement des composantes électroniques un simulateur à impulsions largeur variable est indispensable.



Accession For	
NTIS GRA&I	<input checked="" type="checkbox"/>
DTIC TAB	<input type="checkbox"/>
Unannounced	<input type="checkbox"/>
Justification _____	
By _____	
Distribution/	
Availability Codes	
Dist	Avail and/or Special
A-1	

EXECUTIVE SUMMARY

In order to realistically simulate the effects of the prompt gamma-ray pulse associated with a nuclear weapon on electronics, an electron linear accelerator (LINAC) is often used. The pulse widths available from most LINACs are longer than the typical battlefield pulse. This report examines the effects of varying pulse widths on selected electronic devices summarizing some recent DREO work at a variable pulse-width facility located at Chalk River Nuclear Laboratories.

TABLE OF CONTENTS

	<u>PAGE</u>
ABSTRACT/RÉSUMÉ	ii
EXECUTIVE SUMMARY	iii
TABLE OF CONTENTS	iv
1.0 <u>INTRODUCTION</u>	1
2.0 <u>EXPERIMENTAL</u>	1
2.1 PROPAGATION DELAY TIME IN BIPOLAR TRANSITIONS	1
2.2 SATURATION TIMES IN OP AMPS	4
2.3 CHARGE TRAPPING EFFECTS IN GaAs	5
2.3.1 PULSE WIDTH DEPENDENCE OF CHARGE TRAPPING	5
2.3.2 TEMPERATURE DEPENDENCE OF CHARGE TRAPPING	7
3.0 <u>CONCLUSIONS</u>	9
4.0 <u>BIBLIOGRAPHY</u>	19

TABLES

TABLE 1 Bipolar Transistor Response to Pulse Width Variation.	3
TABLE 2 OPAMP Parameters as Function of Pulse Width	4

FIGURE CAPTIONS

Figure 1	Propagation delay time characteristics of a bipolar transistor showing the components described in the text	10
Figure 2	Measured response of 2N4401 transistor to 80 ns wide pulse. The radiation storage time and fall time parameters are evident	11
Figure 3	Measured response of TIP122 to 350 ns wide pulse. Note that t_{sr} and t_f are greater than for the 2N4401. The increase in t_{sr} was expected due to larger electrical storage time	11
Figure 4	Measured response of 741C operational amplifiers to 84 ns and 2.5 μ s wide pulses, showing wide voltage swings, varying with pulse width	12
Figure 5	Pulse width dependence of positive and negative saturation times for 741C op-amp. Note that the saturation times decrease as the pulse width decreases toward the more realistic value of two shakes	13
Figure 6	Idealized GaAs MESFET response to three pulse widths for traps having time constants of 10 ns, 0.5 μ s and 10 μ s. Note that these effects are truly pulse width - as opposed to dose rate - dependent	14
Figure 7	Realistic predicted GaAs MESFET response to incident square wave irradiations of various pulse widths, incorporating device saturation. Note that in order to observe a particular trap, the pulse width should be similar to the trap time constant	15

Figure 8	Response (lower curve) of NEC270 GaAs MESFET to 3 μ s wide pulse (upper curve). Note the similarity of the response to that predicted - i.e. a saturation which mimics the pulse, followed by an exponential decay due to charge trapping	16
Figure 9	Response of TOS710 MESFET to 2 μ s wide pulse clearly showing superposition of the two effect discussed in the text . . .	17
Figure 10	Response of NEC270 MESFET at two different temperatures, 300 K and 333 K. The enhanced de-trapping at higher temperatures is readily apparent	17
Figure 11	$T^2\tau$ vs $1/T$ plots for both types of MESFETS. From the slopes and intercepts of these plots the trap depths and cross sections can be ascertained as described in the text	18

1.0 INTRODUCTION

The concept of using an electron linear accelerator (LINAC) to simulate the radiation damage in electronics arising from the prompt gamma-ray component of a nuclear burst (causing subsequent photocurrent generation) has been demonstrated valid by many authors (eg 1) and has also been successfully demonstrated by DREO at the Chalk River Nuclear Laboratories (CRNL) 10 MeV LINAC (PHELA) facility (2). The LINAC, as one advantage over a flash X-ray facility, generally offers a variability in pulse widths. Some arguments have been made (3) that dose-rate (photocurrent) effects should be to a large extent pulse-width independent. PHELA was originally capable of 1 μ s to 6 μ s pulse widths, and has recently been modified, under DND contract (4), to change its pulse width range to span 150 ns to 3 μ s. Thus the effects of pulse width, for the same dose rate, could be directly examined.

In view of the fact that recent DREO work has suggested a pulse width of 20 ns (2 shakes) (5) for an actual weapon burst is reasonable - knowledge of this pulse width dependence is essential to the design and subsequent possible purchase of a DREO-based LINAC dedicated to Transient Radiation Effects on Electronics (TREE) work.

The work presented here represents a brief examination of the pulse-width dependence for some of the devices previously tested by DREO. These results represent only one day's work at PHELA due to severe time constraints, however some interesting trends are observed.

2.0 EXPERIMENTAL

2.1 Propagation Delay Time in Bipolar Transitions

One area in which a definite pulse width effect has been noted is in the propagation delay time in bipolar transistors caused by the radiation pulse. Following along the lines of the discussion in Messenger and Ash (6), this propagation delay time t_p is given (see Fig. 1) as

$$t_p = t_d + t_r + t_{sr} + t_f \quad (1)$$

where t_d = delay time to bring device from its on state to 10% of saturation current

t_r = rise time to 90% of saturation

t_{sr} = time device spends in saturation following pulse cessation (radiation storage time)

and t_f = fall time back to 10% of saturated current.

Of these, t_{sr} has shown some pulse width dependence as (1)

$$t_{sr} = t_s \ln \{ K_1 (1 - e^{-t_p/0.3t_s}) - K_2 \} \quad (2)$$

where t_s = electrical storage time

t_p = pulse width

and K_1 and K_2 are device dependent constants.

Messenger and Ash imply no direct pulse width dependence in the remaining three terms of equation 1.

In order to examine these trends, two bipolar transistor types were exposed to varying pulse widths, for the same dose rate ($\dot{\gamma} \approx 3 \times 10^9$ Rads (Si)/s). They were 2N4401 ($t_s = 225$ ns) and TIP122 ($t_s = 8.5 \mu\text{s}$) (where the electrical storage times are from the manufacturers). Examples of their measured responses to LINAC pulses appear in Figs. 2 and 3 respectively. To expedite data analysis, a Tektronics 230 oscilloscope output of device response was fed to a PC (in LOTUS format) enabling accurate analysis simply by numerical interpolation of the LOTUS files. The results of these analyses appear in Table 1.

Immediately obvious is the previously observed (2) proportionality between radiation storage time and electrical storage time. Explicitly the ratios are in somewhat reasonable agreement at:

$$\frac{(t_{sr})_{2N4401}}{(t_{sr})_{TIP122}} = 1.04 \times 10^{-1} \quad (3)$$

and

$$\frac{(t_s)_{2N4401}}{(t_s)_{TIP122}} = 2.65 \times 10^{-2} \quad (4)$$

As shown in table 1, for both transistors studied here, all parameters proved to be pulse-width independent - within

experimental error. (Note that t_d and t_r are not evaluated for the TIP122 transistor due to the fact that this device proved sensitive to the (6 μ s) RF pulse associated with the electron pulse. However, in view of the very fast rise time at the actual pulse arrival, it is felt that t_d and t_r are both insignificant in comparison to t_{sr}). For these two cases then, LINAC testing at virtually any pulse width should yield reliable results when extrapolated to the battlefield timeframe.

Table 1

Bipolar Transistor Response To Pulse Width Variation (Dose Rate - 3×10^9 Rads(Si)/s)

(a) 2N4401 ($t_s = 225$ ns)

LINAC Pulse Width

(ns) (FWHM)	t_d (ns)	t_r (ns)	t_{sr} (ns)	t_f (ns)	t_p (ns)
1600±100	<10	50±5	950±100	390±50	1400±110
540±50	<10	50±5	1054±100	300±50	1414±110
283±20	<10	50±5	1132±100	360±50	1552±110
137±10	<10	50±5	1083±100	470±50	1553±110
78±5	<10	50±5	1064±100	380±50	1504±110

(b) TIP122 ($t_s = 8.5$ ns)

LINAC Pulse Width

(ns) (FWHM)	t_d (ns)	t_r (ns)	t_{sr} (μ s)	t_f (μ s)	t_p (μ s)
1600±100	-	-	9.6±0.1	4.3±0.1	13.9±0.1
350±30	-	-	9.5±0.1	4.4±0.1	13.9±0.1

2.2 Saturation Times in OP AMPS

A 741C operational amplifier was powered and biased, with gain of 100, and exposed to various pulse widths (dose rate $\sim 7 \times 10^8$ Rads (Si)/s). The measurement circuit used here was the same as reported in previous DREO work (2). Typical responses are shown in Fig. 4. Note the alternate negative and positive saturations typical of op-amp dose-rate performance. The time the device spends at the negative and positive rails as a function of pulse width appears in Table 2.

Table 2
741C OP-AMP Parameters as Function of Pulse Width

LINAC Pulse Width (ns) ($\pm 10\%$)	Time At Negative Rail (μ s) ($\pm .1\mu$ s)	Time At Positive Rail (μ s) ($\pm .1\mu$ s)
2500	5.1	10.5
1500	5.0	10.0
650	4.3	10.0
500	4.3	9.4
430	4.4	9.3
200	4.1	9.0
112	3.7	5.0
84	3.4	4.5

There is a large pulse width-dependent effect in this particular op-amp. The response of the op-amp may be considered to be dominated by (bipolar) transistors being driven into saturation and subsequent on-board amplification. Thus there would seem to be definite evidence for a radiation storage time dependence on pulse width for the transistors used in this op-amp. Extrapolation down to the two shake pulse width would give positive and negative saturation times of less than 1μ s. (see Fig. (5)). So when designing/building circuitry capable of withstanding the op-amp radiation-induced voltage swings produced by μ s wide pulses, protection against the actual (20 ns) induced swings will be achieved but will result in much unnecessary over-design (and accompanying cost). The op-amp is an example of a device which must be tested in the expected battlefield timeframe.

2.3 Charge Trapping Effects in GaAs

Charge trapping is the withholding of normal charge motion in a material for any number of physical reasons. In the case of GaAs MESFETS, electron charge trapping near the FET channel region has been observed by numerous authors (eg 2,7,8).

For the case of a LINAC pulse irradiating a GaAs device, electron hole pairs are created by the pulse, however the electrons may be trapped at an energy level E_T below the conduction band. These electrons may then decay from this level with a characteristic time constant depending upon, among other factors, trap depth and temperature as discussed later in this section.

2.3.1 Pulse Width Dependence of Charge Trapping

This immediate discussion centres on the pulse width dependence of charge trapping. Although the total number of electrons which are trapped at any level for a given irradiation is directly proportional to incident radiation fluence, the timeframe over which the radiation is given is also a key factor in the determination of this parameter. The radiation pulse width will determine which traps (corresponding to a particular time constant) will be preferentially filled - and subsequently emptied. Thus the radiation pulse width will determine whether or not a specific charge trapping reaction may be experimentally observed.

The mathematical and pictorial analysis below should clarify this, however as a rough rule of thumb in order to observe a trap with a characteristic time constant τ , the radiation pulse width must be at maximum of the order of τ . This explains why charge trapping effects are impossible to observe with steady state radiation as no trap depths corresponding to very long time constants are possible (due to very large E_T exceeding the conduction band gap).

MacLean, in his excellent review article on MOS devices (9), has referred to short-pulse charge trapping as an apparent dose rate effect. We consider this terminology to be somewhat misleading as dose rate effects usually refer to photocurrent generation, which is not a factor in the charge trapping mechanisms. Rather the terminology "pulse-width dependent ionization effects" is proposed as a more accurate description.

In order to mathematically simulate the charge trapping and decay mechanisms we use a simple mathematical approach. Since the traps are observed to have a characteristic time constant, then the trapping and de-trapping may be expressed by simple exponential functions - analogous to neutron capture and radiative decay for a constant steady-state fluence.

$$N(t) \propto \phi(E) \sigma(E) (1 - e^{-t/\tau}); \quad t < t_w \quad (5)$$

$$N(t) \propto N(t_w) e^{-t/\tau}; \quad t > t_w \quad (6)$$

where $N(t)$ = number of electrons in trap at energy E_T
 $\phi(E)$ = energy fluence of incident radiation
 $\sigma(E)$ = energy-dependent trapping cross section
 τ = characteristic time constant of the trap
 t_w = radiation pulse width
 $N(t_w)$ = number of traps filled at $t=t_w$

Of course photocurrents will also be generated due to the high dose rates. For high electron mobility devices such as GaAs, one need not consider the diffusion component of photocurrent, but only the drift component (i.e. neglect radiation storage time). Then the photocurrent component will mirror the radiation pulse $P(t)$ giving the total transistor response $R(t)$ as,

$$R(t) = N(t) + C P(t) \quad t < t_w \quad (7)$$

$$R(t) = N(t) \quad t > t_w \quad (8)$$

where C = proportionality constant

Now, consider the case where more than one trap is filled, each having its own characteristic time constant τ_i then

$$R(t) \propto C P(t) + \phi(E) \sigma(E) \sum_i (1 - \exp(-t/\tau_i)); \quad t < t_w \quad (9)$$

$$R(t) \propto N(t_w) \sum_i \exp(-t/\tau_i); \quad t > t_w \quad (10)$$

To simplify the above expressions, consider the cases of three traps with time constants of 10 ns, 1 μ s and 100 μ s (one should note that the cited literature has observed trapping time constants from a few ns to 70 s). As an "idealized" response we first consider C vanishingly small, and thus the first term in

eq'n 9 to be insignificant when compared to the second. For simplicity we also set $\phi = \sigma = 1$. The total idealized response for pulse widths of 10 ns, 0.5 μ s and 10 μ s is given in Fig. 6. Note the vast difference in recovery time for the three cases, dictating which trap levels may be observed.

Now, for a more realistic case, we allow the transistor to be driven into saturation very quickly by the pulse and held there until pulse cessation. Stating this another way, since there are many more states in the conduction band than traps, then photocurrent generation will always dominate, obscuring trapping and allowing only (post pulse) de-trapping to be observed. This modification, for square wave pulses, results in the possible responses in Fig. 7 (Here the saturation levels have been shifted to allow easier observation of the effects). Note the sharp drop-off immediately after the pulse followed by exponential decay. Fig. 8 (from (2)) shows this behaviour experimentally, i.e. the device mimics the pulse until the value of $N_{(tw)}$ is reached, when charge de-trapping occurs.

Fig. 9 show the response of the TOS710 MESFET to a 2 μ s wide LINAC pulse, as discussed later. Clearly contributions from charge de-trapping and the very fast GaAs photocurrent generation are observed.

Thus to predict the behaviour of GaAs devices on the battlefield, it is imperative that an accurate pulse width be employed in any simulator. However, to completely understand the nature and origin of trapping in GaAs, a variety of pulse widths is necessary. A variable pulse width LINAC is essential then, to understand all possible reactions.

2.3.2 Temperature Dependence of Charge Trapping

The PHELA experiments conducted for this work also involved an analysis of the temperature dependence of trapped charge decay in two GaAs MESFETS - the NEC 270 and TOS710. The temperature was controlled both during and after the radiation pulse by the use of a TATS 400 (10) control system. A thermostat was placed near the device to achieve accurate readout. In order to minimize the number of interfering traps and stay within time

constraints, only one pulse width was used. This was the longest possible ($\sim 2\mu\text{s}$) at the closest possible distance (20cm) to the beam exit window in order to maximize total dose and guarantee maximum possible trapping.

Consider, for simplicity, only one single trap (or one dominant trap) corresponding to one single energy level at depth E_T below the conduction band. Then one may write the post-irradiation emission probability, p , from the E_T trap (at any temperature T) as

$$p = \sigma V_{th} N_c \exp [- E_T/kT] \quad (11)$$

where σ = capture cross section

k = Boltzman's constant

V_{th} = thermal velocity of electrons

and N_c = effective density of electron states in the conduction band

The associated emission lifetime from E_T is simply

$$\tau = 1/p = [\sigma v_{th} N_c]^{-1} \exp (E_T/kT) \quad (12)$$

If the constants in square brackets were completely temperature independent then a semi-log plot of τ vs $1/T$ would yield E_T . However, only the trapping cross-section satisfies this criterion. The others may be evaluated from (6)

$$V_{th} = [3kT/m]^{1/2} \text{ and } N_c = 2/h^3 (2\pi m kT)^{3/2} \quad (13)$$

where m = electron mass

h = Planck's constant

Substituting into eq'n 12 then the result is

$$T^2 \tau = (1/\sigma A) \exp [E_T/kT] \quad (14)$$

where $A =$ temperature independent constant $\approx 54.6 \text{ k}^2\text{m/h}^3$

Thus plotting (semi-log) $T^2 \tau$ vs $1/T$ will give the trapping depth E_T from the slope, and σ from the intercept.

This analysis was used on the data from the PHELA work. The temperature dependence of the emission lifetime is clearly evident in Fig. 10 for the NEC 270 device. Fig. (11) shows the $T^2\tau$ plots for the two devices. From the slopes, the evaluated trap depths are $E_T = (0.3 \pm .02) \text{ eV}$ for the NEC 270 device and $E_T = (0.09 \pm .02) \text{ eV}$ for the TOS710 device. Bellem (8) has done extensive investigations on charge trapping in GaAs CCD devices, and has reported trap levels at 0.36 eV (labelled E3 or EL5) and 0.1 eV (labelled E1), in good agreement with the values reported here.

The associated cross section analysis would yield extremely low values of $\sim 10^{-19} \text{ cm}^2$ for both devices.

The room temperature de-trapping time constants for the two devices were 330 μs for the NEC 270 and 105 μs for the TOS710.

3.0 CONCLUSIONS

The use of accurate pulse widths to simulate the prompt component of a nuclear weapon burst has proven to be of great importance for a number of devices. It is suggested that any DREO - based machine have the capabilities to span a wide range of pulse widths, with a 20 ns wide pulse being of prime importance. A span of 10 ns to 10 μs would be extremely useful, provided the same dose rate is available for all widths.

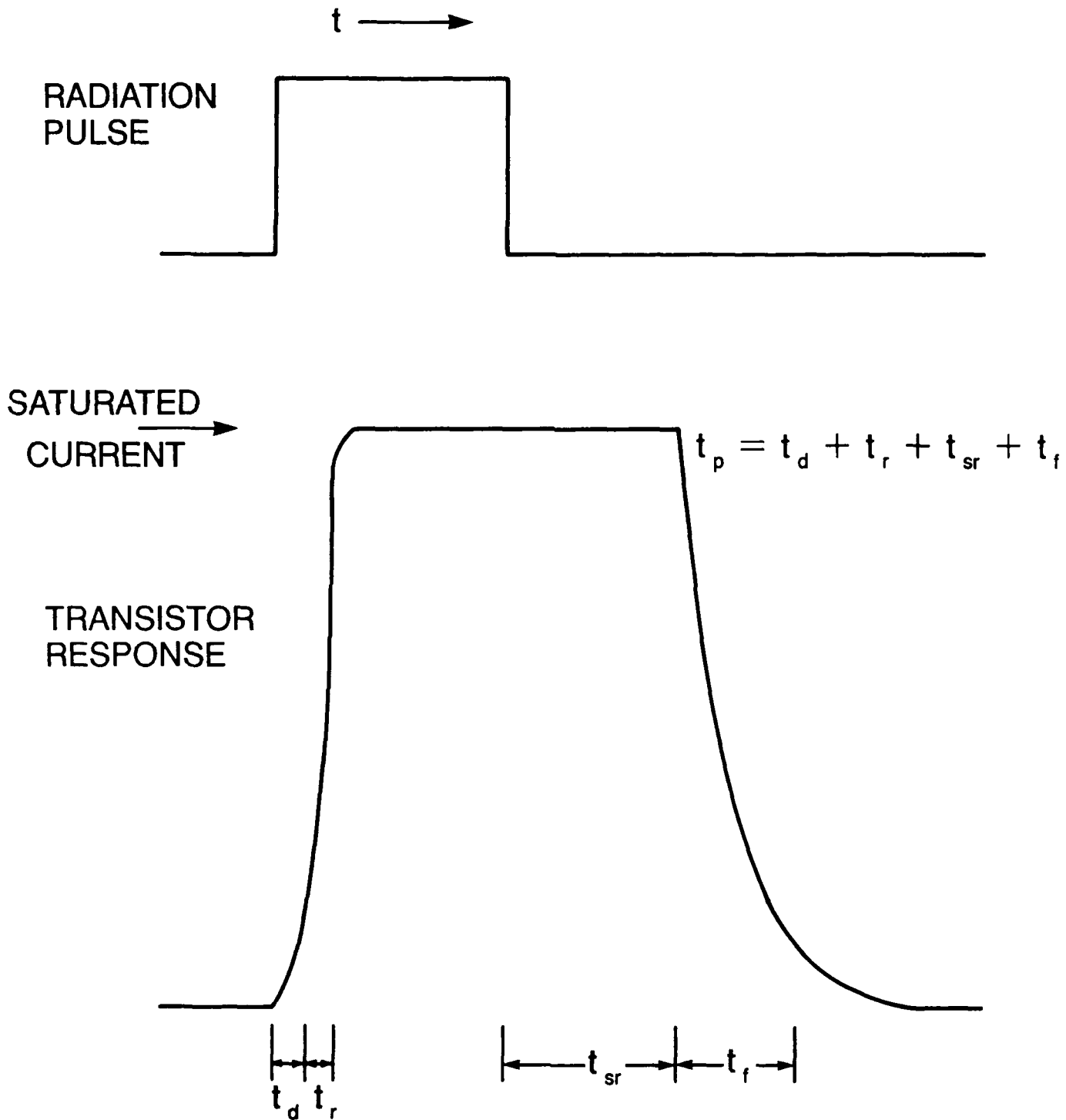


Figure 1 Propagation delay time characteristics of a bipolar transistor showing the components described in the text

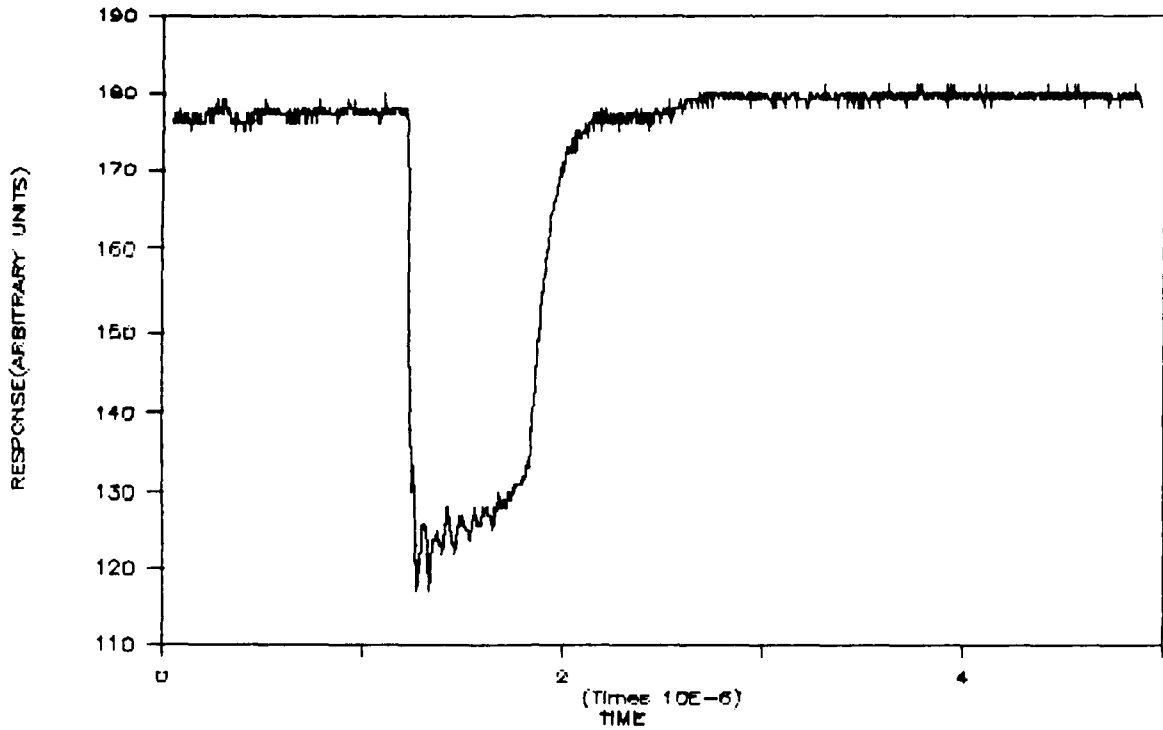


Figure 2 Measured response of 2N4401 transistor to 80 ns wide pulse. The radiation storage time and fall time parameters are evident

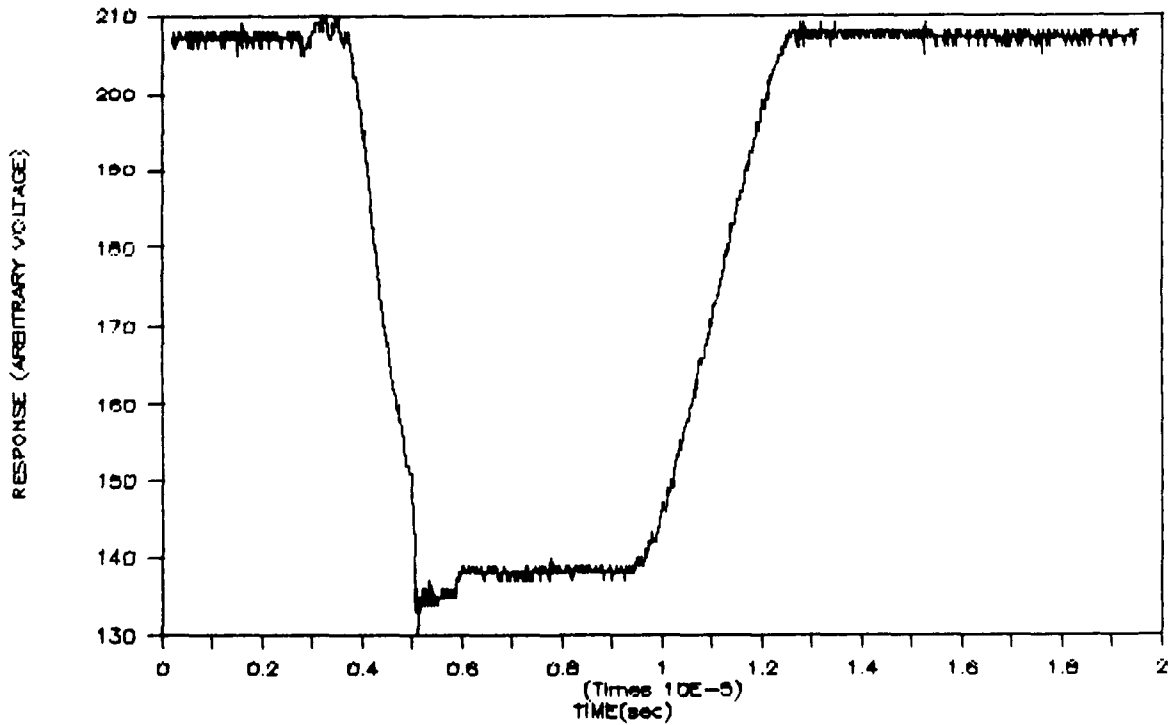


Figure 3 Measured response of TIP122 to 350 ns wide pulse. Note that t_{sr} and t_f are greater than for the 2N4401. The increase in t_{sr} was expected due to large electrical storage time

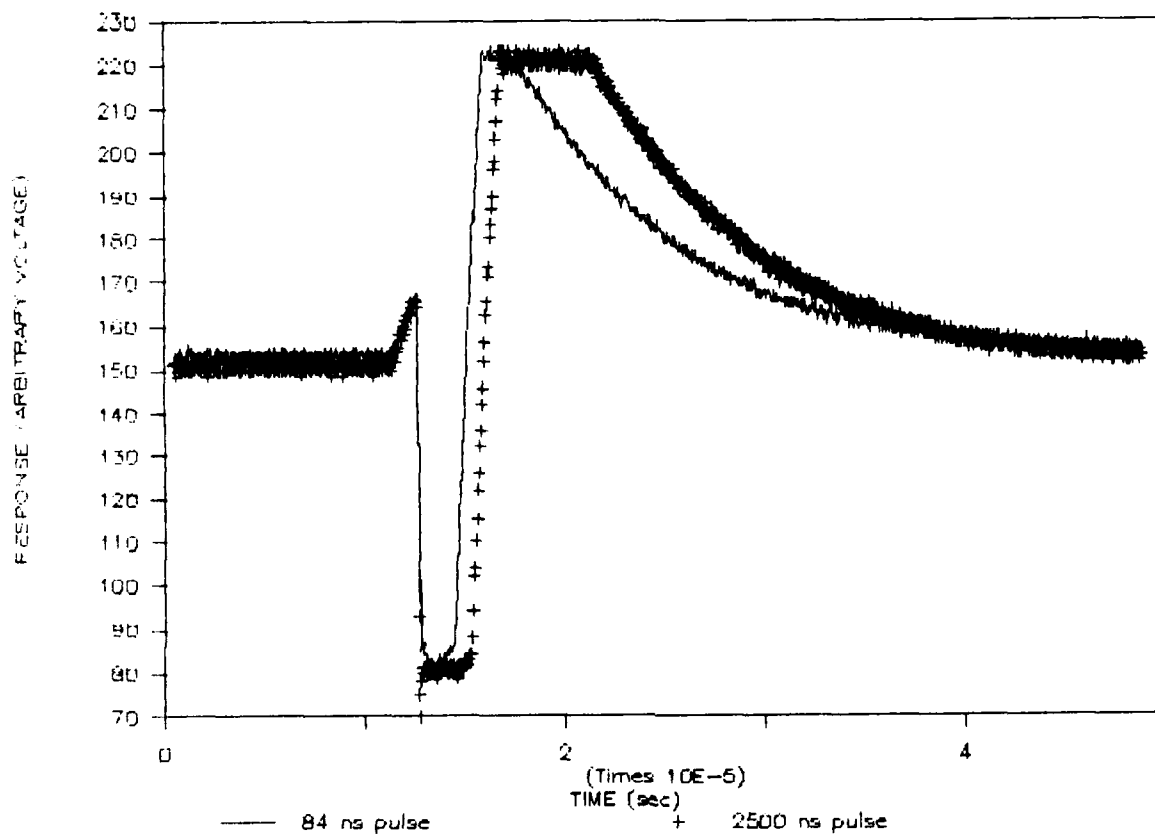


Figure 4 Measured response of 741C operational amplifiers to 84 ns and 2.5 μ s wide pulses, showing wide voltage swings, varying with pulse width

741C OPAMP RESPONSE VARIOUS PULSE WIDTHS

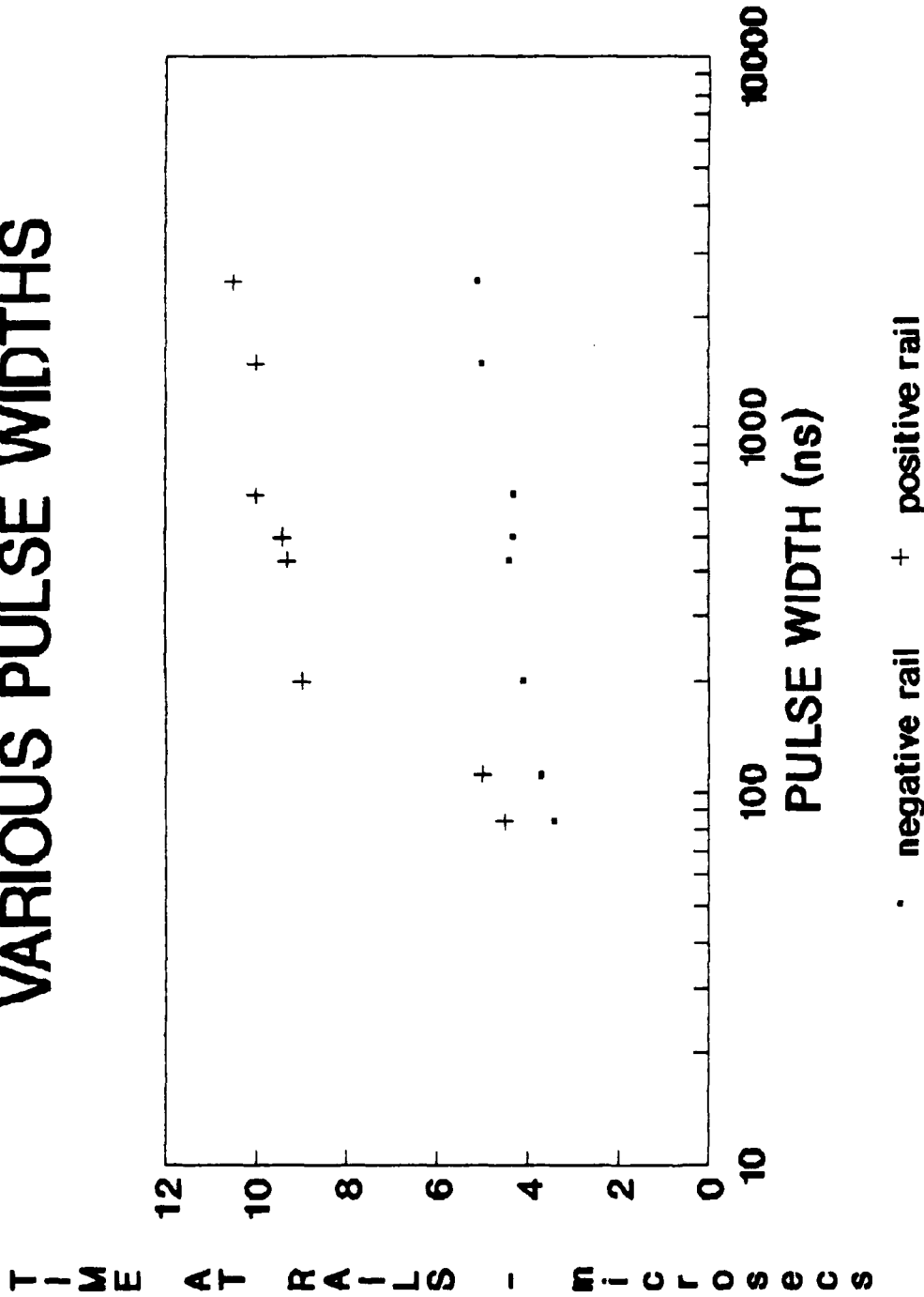


Figure 5 Pulse width dependence of positive and negative saturation times for 741C op-amp
Note that the saturation times decrease as the pulse decreases toward the more realistic value of two shakes

GaAs idealized response various pulse widths

MESFET response - arbitrary units

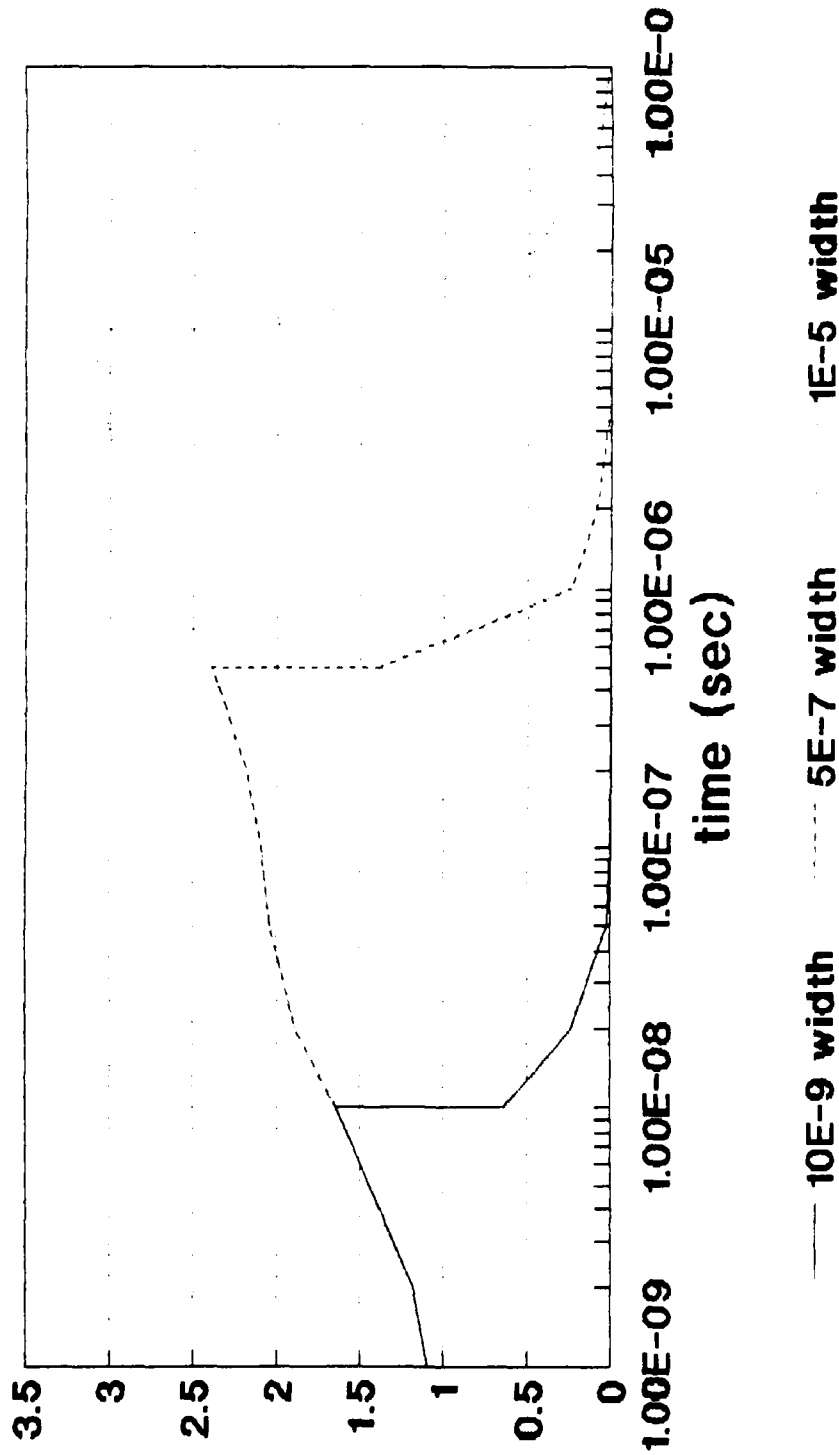


Figure 6 Idealized GaAs MESFET response to three pulse width for traps having time constants of 10 ns, 0.5 μ s and 10 μ s. Note that these effects are truly pulse width - as opposed to dose rate - dependent

GaAs saturated response various pulse widths

MESFET response - arbitrary units

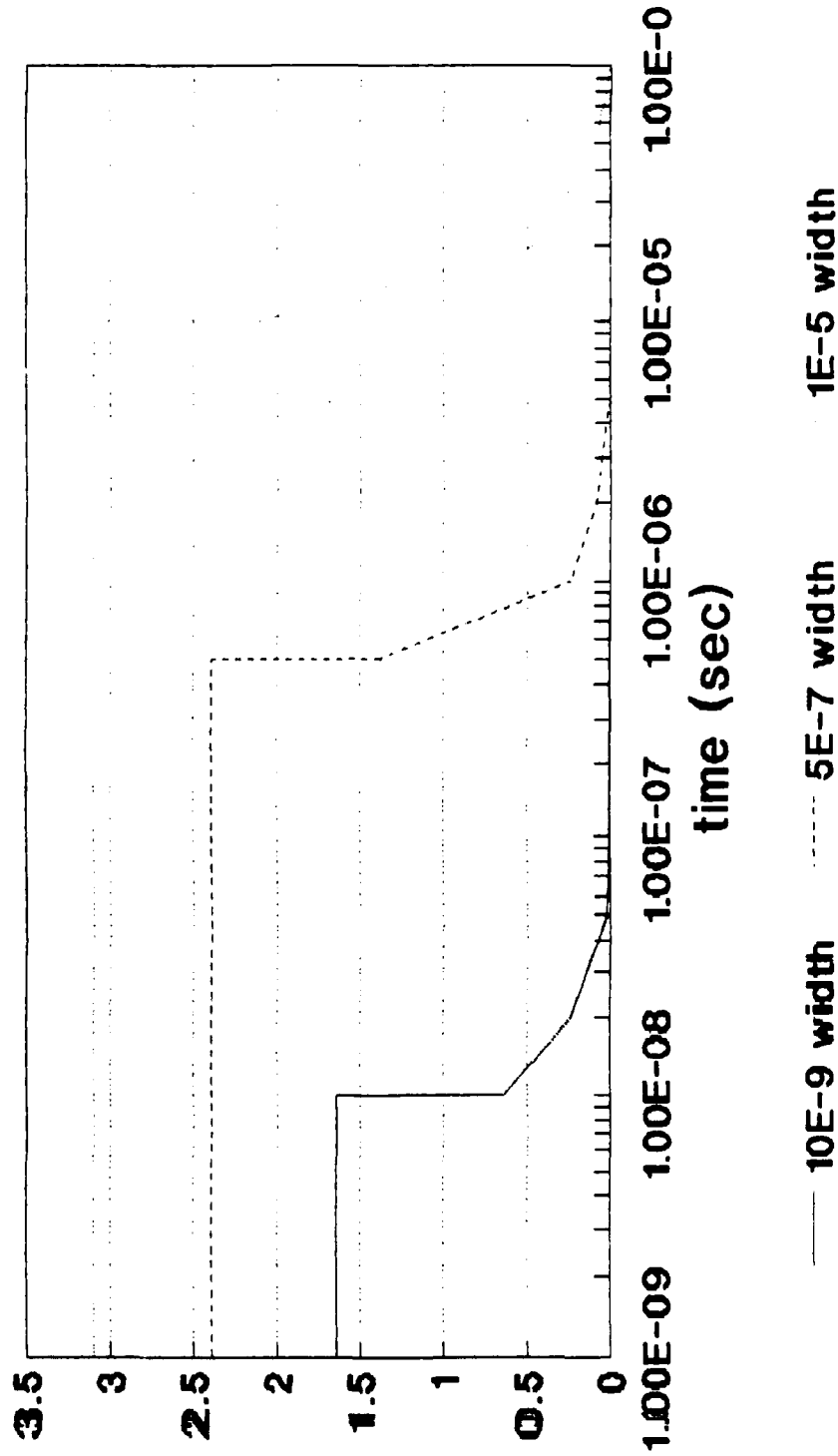


Figure 7 Realistic predicted GaAs MESFET response to incident square wave irradiations of various pulse widths, incorporating device saturation. Note that in order to observe a particular trap, the pulse width should be similar to the trap time constant

CH1 100mV 5 A 2us -46.9mV EXT1
CH2 500mV500HM

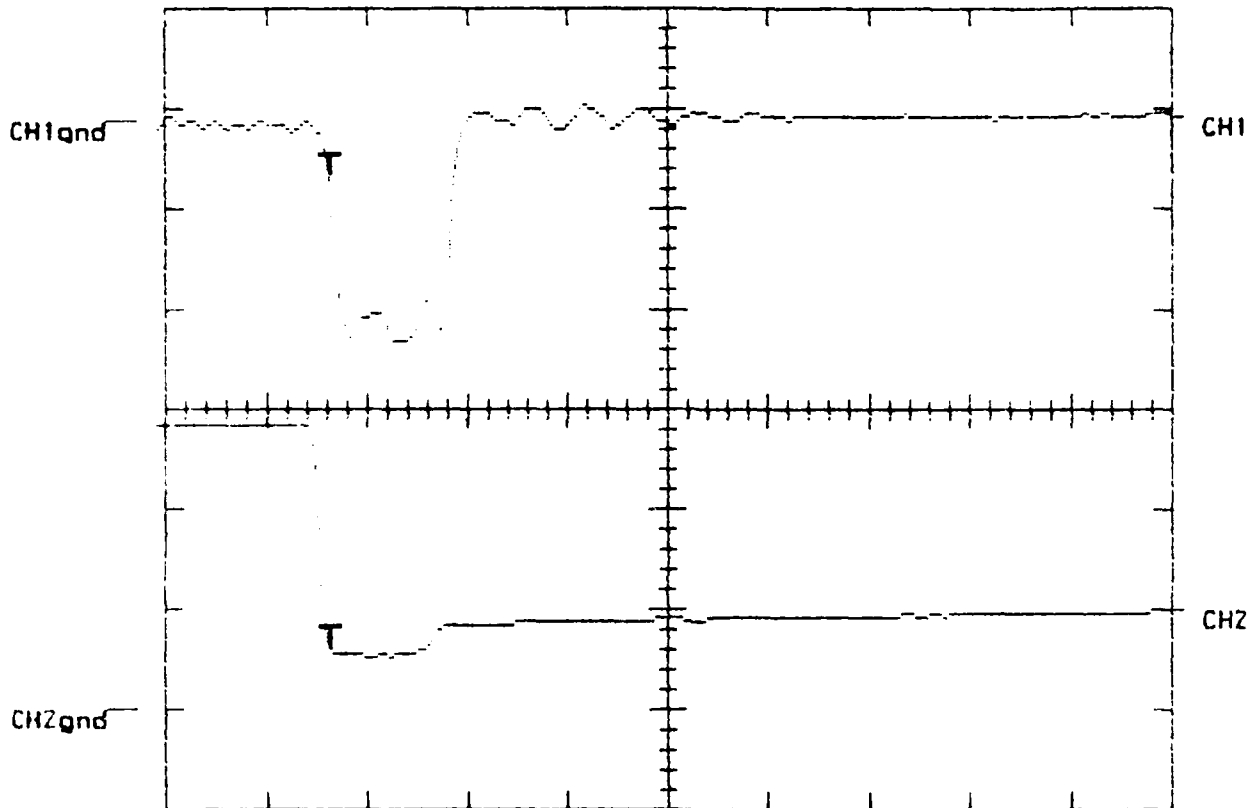


Figure 8 Response (lower curve) of NEC270 GaAs MESFET 3 μ s wide pulse (upper curve). Note the similarity of the response to that predicted - i.e. a saturation which mimics the pulse, followed by an exponential decay due to charge trapping

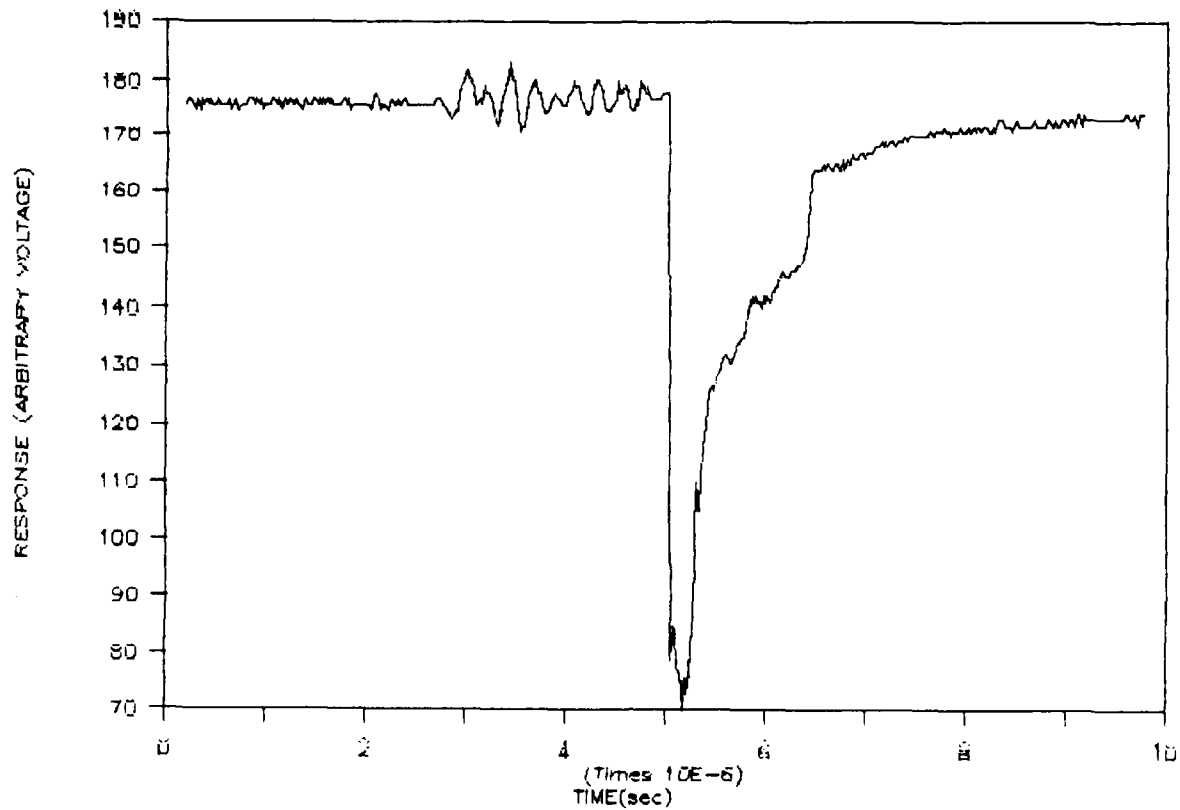


Figure 9 Response of TOS710 MESFET to 2 μs wide pulse clearly showing superposition of the two effect discussed in the text

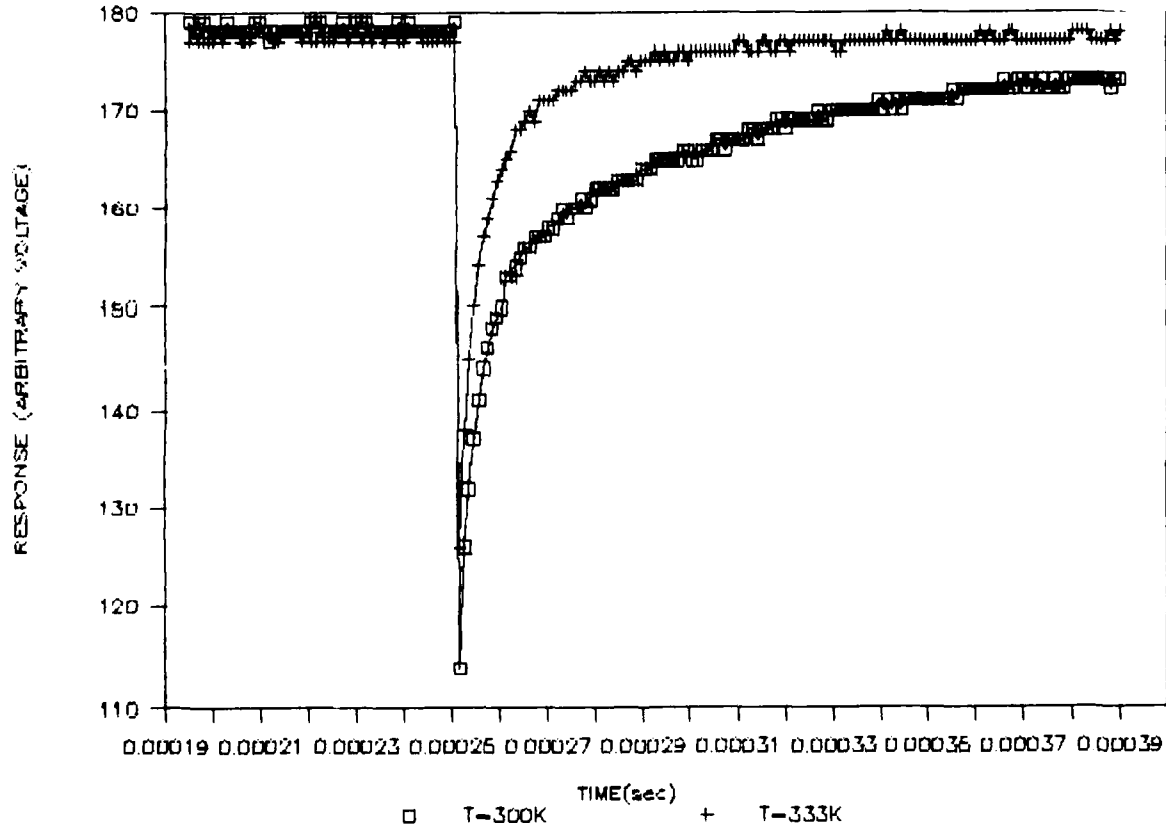


Figure 10 Response of NEC270 MESFET at two different temperatures, 300 K and 333K. The enhanced de-trapping at higher temperatures is readily apparent

TEMPERATURE DEPENDENCE OF GaAs DEVICES

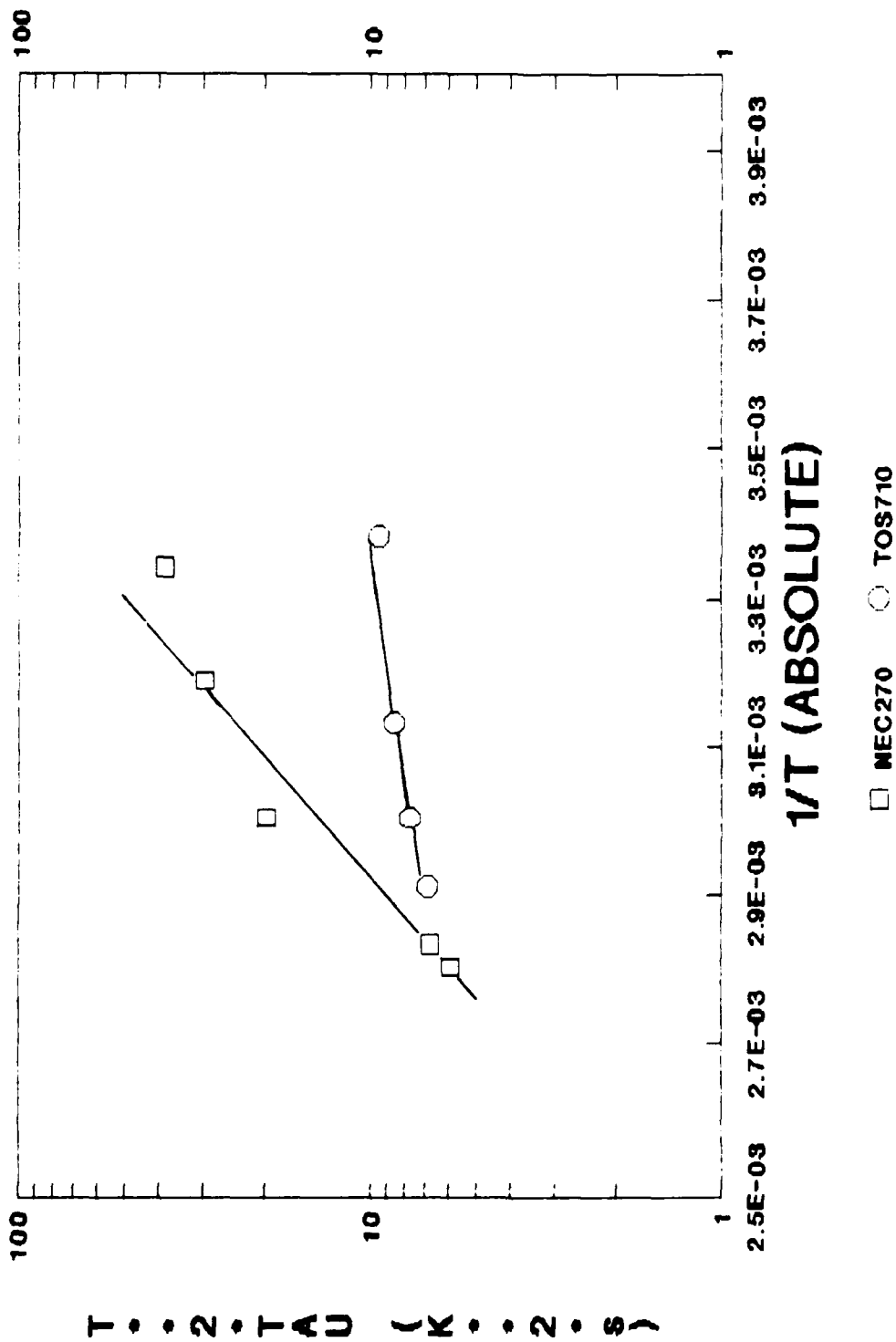


Figure 11 $T^2\tau$ vs $1/\tau$ plots for both types of MESFETS. From the slopes and intercepts of these plots the trap depths and cross sections can be ascertained as described in the text

4.0 REFERENCES

- 1) Harrity J.W. and P.E. Gammill "Upset and Latchup Thresholds in CD 4000 Series of CMOS devices", IEEE Annual Conference on Nuclear and Space Radiation Effects, Cornell University, Ithaca, N.Y., July 1980.
- 2) Cousins T. and B.E. Hoffarth, "The Measured Response of Selected Electronic Components to Fast Pulse Electrons (U)", DREO Technical Note 88-13, May 1988 (confidential).
- 3) IRT Corporation Report #4251-009, "Guidelines for Radiation Effects Testing", IRT Corporation, 1978.
- 4) Cousins T. and R.A. Gravelle, DREO Trip Report "Visit to Chalk River Nuclear Laboratories PHELA Facility, 02-03 February 1989", 14 February 1989.
- 5) Cousins T. "The Use of the Computer Code ATR to Relate DREO Experimental Results to Nuclear Battlefield Threats", DREO Technical Note (in press).
- 6) Messenger G.C. and M.S. Ash, "The Effects of Radiation on Electronic Systems", Von Nostrand Reinhold Company, N.Y., 1986.
- 7) Simons M. and E.E. King, "Long Term Radiation Transients in GaAs FETS", IEEE Trans. Nuc. Sci., Vol NS 26, No. 6, 1979, pp. 5080-5086.
- 8) Bellem R.D. and W.C. Jenkins, "Radiation Effects on GaAs charge coupled devices with high resistivity gate structures", IEEE Trans. Nuc. Sci., Vol NS-33, No. 4, 1986, pp. 1084-1089.
- 9) MacLean F.B. and T.R. Oldham "Total Dose Ionization Effects" IEEE Trans. Nuc. Sci. Short Course Notes, 1987.
- 10) Tausch H.J., R. Wemhoner, R.L. Pease, J.R. Schwork and R.J. Maier, "A Programmable Test System for Transient Annealing Characterization of Irradiated Mosfets" IEEE Trans. Nuc. Sci., Vol NS-34, No. 6, 1987 pp. 1763-1768.

SECURITY CLASSIFICATION OF FORM
(highest classification of Title, Abstract, Keywords)

DOCUMENT CONTROL DATA

(Security classification of title, body of abstract and indexing annotation must be entered when the overall document is classified)

<p>1. ORIGINATOR (the name and address of the organization preparing the document. Organizations for whom the document was prepared, e.g. Establishment sponsoring a contractor's report, or tasking agency, are entered in section 8.)</p> <p>Defence Research Establishment Ottawa Ottawa, Ontario K1A 0Z4</p>	<p>2. SECURITY CLASSIFICATION (overall security classification of the document, including special warning terms if applicable)</p> <p style="text-align: center;">UNCLASSIFIED</p>	
<p>3. TITLE (the complete document title as indicated on the title page. Its classification should be indicated by the appropriate abbreviation (S.C.R or U) in parentheses after the title.)</p> <p style="text-align: center;">Pulse-Width Dependent Radiation Effects on Electronic Components (U)</p>		
<p>4. AUTHORS (Last name, first name, middle initial)</p> <p style="text-align: center;">Cousins, Thomas</p>		
<p>5. DATE OF PUBLICATION (month and year of publication of document)</p> <p style="text-align: center;">October 1989</p>	<p>6a. NO OF PAGES (total containing information. Include Annexes, Appendices, etc.)</p> <p style="text-align: center;">19</p>	<p>6b. NO OF REFS (total cited in document)</p> <p style="text-align: center;">10</p>
<p>7. DESCRIPTIVE NOTES (the category of the document, e.g. technical report, technical note or memorandum. If appropriate, enter the type of report, e.g. interim, progress, summary, annual or final. Give the inclusive dates when a specific reporting period is covered.)</p> <p style="text-align: center;">Technical Note</p>		
<p>8. SPONSORING ACTIVITY (the name of the department project office or laboratory sponsoring the research and development. Include the address.)</p> <p>Defence Research Establishment Ottawa Ottawa, Ontario K1A 0Z4</p>		
<p>9a. PROJECT OR GRANT NO. (if appropriate, the applicable research and development project or grant number under which the document was written. Please specify whether project or grant)</p> <p style="text-align: center;">041LS</p>	<p>9b. CONTRACT NO. (if appropriate, the applicable number under which the document was written)</p>	
<p>10a. ORIGINATOR'S DOCUMENT NUMBER (the official document number by which the document is identified by the originating activity. This number must be unique to this document.)</p> <p style="text-align: center;">DREO TECHNICAL NOTE 89-33</p>	<p>10b. OTHER DOCUMENT NOS. (Any other numbers which may be assigned this document either by the originator or by the sponsor)</p>	
<p>11. DOCUMENT AVAILABILITY (any limitations on further dissemination of the document, other than those imposed by security classification)</p> <p>(X) Unlimited distribution () Distribution limited to defence departments and defence contractors; further distribution only as approved () Distribution limited to defence departments and Canadian defence contractors; further distribution only as approved () Distribution limited to government departments and agencies; further distribution only as approved () Distribution limited to defence departments; further distribution only as approved () Other (please specify):</p>		
<p>12. DOCUMENT ANNOUNCEMENT (any limitation to the bibliographic announcement of this document. This will normally correspond to the Document Availability (11). However, where further distribution (beyond the audience specified in 11) is possible, a wider announcement audience may be selected.)</p>		

13. ABSTRACT (a brief and factual summary of the document. It may also appear elsewhere in the body of the document itself. It is highly desirable that the abstract of classified documents be unclassified. Each paragraph of the abstract shall begin with an indication of the security classification of the information in the paragraph (unless the document itself is unclassified) represented as (S), (C), (R), or (U). It is not necessary to include here abstracts in both official languages unless the text is bilingual).

The simulation of the prompt gamma-ray pulse effects on electronics with an electron linear accelerator (LINAC) has been performed by DREO and other groups. However, the use of a LINAC normally entails wider pulses than those expected on the battlefield. This report examines the effects of the variation of pulse width on electronic response using both theoretical and experimental examples. The conclusions are that pulse-width fidelity is important for a number of possible scenarios, and that for complete understanding of electronic performance, a variable pulse-width simulator is essential.

14. KEYWORDS, DESCRIPTORS or IDENTIFIERS (technically meaningful terms or short phrases that characterize a document and could be helpful in cataloguing the document. They should be selected so that no security classification is required. Identifiers, such as equipment model designation, trade name, military project code name, geographic location may also be included, if possible keywords should be selected from a published thesaurus, e.g. Thesaurus of Engineering and Scientific Terms (TEST) and that thesaurus-identified. If it is not possible to select indexing terms which are Unclassified, the classification of each should be indicated as with the title.)

Transient Radiation Effects on Electronics
Electron Linear Accelerator
Radiation Dose Rate
Electron Pulse Width
Biopolar Transistors
Op-Amp
Gallium Arsenide
Charge Trapping